Decoupling Between Two Conductor Microstrip Transmission Line

Shidong He, Atef Z. Elsherbeni, *Senior Member, IEEE,* and Charles E. Smith, *Senior Member, IEEE*

***Abstract*—A numerical analysis of two-conductor transmission line with a rectangular notch in the dielectric between the strips is presented. Three media integral equations are derived and solved for the charge distributions. The decoupling between such two-conductor coupled microstrip transmission line is investigated for asymmetric conductors. It is found that the coupling between two conducting lines can be reduced significantly by removing dielectric material between the lines which has a rectangular shape. For best decoupling, the width should be as wide as possible between the conducting lines but the depth should have an optima somewhere in the base dielectric substrate.**

I. Introduction

IN THE LAST two decades, with the development of electronic hardware, the trend of design has shifted from dependence on both electrically and physically large components, which are more independent of each other, to universal usage of smaller and denser integrated circuits and systems which are more tightly coupled. This appears to be continuing along with the requirement for faster circuits and larger bandwidth. With the universal use of smaller and denser circuits, the operation of systems becomes much more dependent on how signals propagate on the circuit interconnections. The related coupling between circuit interconnections limits the bandwidth of dense microwave circuits and the logic speed of digital and computing circuits and systems. Previous study has been devoted to characterize this circuit behavior based on planar infinite-width substrate models [1]. However, it is extremely important to find a practical method to minimize the coupling between interconnecting lines.

In this investigation, attention is focused on the problem of decoupling between a two-conductor microstrip transmission line. One possible method is by employing a rectangular dielectric notch between the two conducting lines as shown in Fig. 1. The reduction of inter-line coupling can be accomplished by possible changes in the dimensions of the notch and the relative permittivites of the substrate and notch region.

The transmission line problem shown in Fig. 1 can be solved using a free-space Green's function formulation in terms of equivalent surface charge sources coupled with a moment method solution [2] using a quasistatic TEM model. This approach to planar type problems has been described by Harrington and Pontoppidan [3], Adams and Mautz [4], and, in a slightly different form, by Smith [5] and Smith and Chang [6], [7]. A method for computing the normal mode parameters of asymmetric coupled microstrip lines is developed in [8]. Coupled integral equations are formed and solved for the self and mutual capacitances of asymmetric

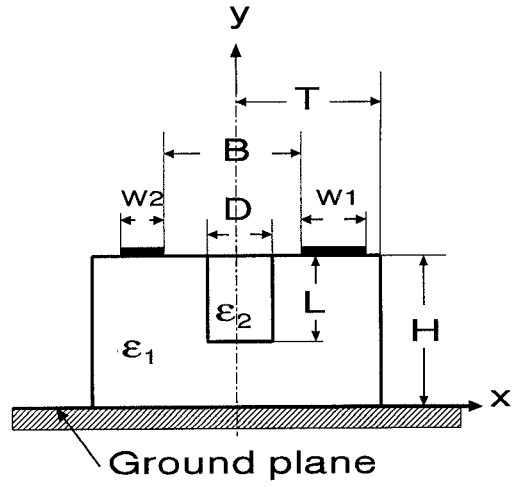

Fig. 1. Cross-section of the two-conductor microstrip transmission line.

lines by moment methods. The asymmetric transmission lines with finite length are discussed by Tripathi [9]. Terminal characteristic parameters (impedance, admittance, etc.) are derived in terms of two independent modes that propagate in two uniformly coupled propagating systems. The theory of quasi-TEM modes on coupled transmission lines in terms of voltage and current eigenvectors is developed by Kajfez [10], [11]. It has been shown that the even and odd modes are possible only when the coupled transmission line is of symmetric shape.

In this paper, integral equations in terms of equivalent charges and a free-space Green's function are derived by enforcing the proper boundary conditions. Here, an ideal model is considered, where the conductors are assumed to be perfect, the dielectric materials are assumed to be lossless isotropic and homogeneous and the thickness of the conductor is assumed to be zero. The formulation used in this study is similar to those in [5]–[7], however it is applied here for a slightly more complicated geometry. An attempt is made to find a method to reduce the coupling between two-conductor microstrip transmission line.

II. Basic Formulation

The integral equations related to this study are developed by considering a two-dimensional boundary value problem. The equations to be derived are valid for the general case of three dielectric regions with perfectly conducting strips inside one of these dielectric regions, as shown in Fig. 2. Region I consists of a dielectric material of permittivity ϵ_1, bounded by

0018–9480/93$03.00 © 1993 IEEE

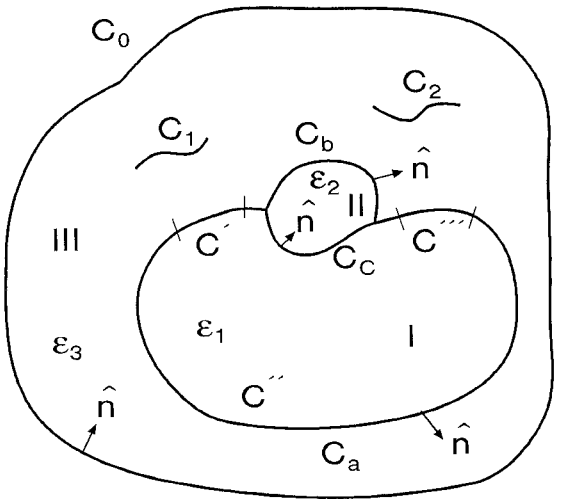

Fig. 2. Generalized static problem.

contours C_a and C_c where $C_a = C' + C'' + C''''$. Region II consists of a dielectric material with permittivity ϵ_2, bounded by contours C_b and C_c. Region III consists of a dielectric material with permittivity ϵ_3, bounded by contours C_a, C_b, C_0 and $C_t = C_a + C_b + C_c$. Inside region III there are two perfectly conducting strips C_1 and C_2 with surface charges ρ_{s1} and ρ_{s2}. The potentials ϕ_{C0}, ϕ_{C1} and ϕ_{C2} are known and are constant on C_0, C_1, and C_2, respectively. However, neither ϕ nor $\partial\phi/\partial n$ are known on C_a, C_b and C_c.

Laplace's equation in the source-free region I is given by

$$\nabla^2\phi_1(x,y) = 0, \tag{1}$$

where the free-space Green's function region

$$\nabla^2 G_0(x,y;x',y') = -\delta(x,y;x',y'), \tag{2}$$

can be considered with

$$G_0(x,y;x',y') = \frac{1}{2\pi}\ln\frac{1}{[(x-x')^2+(y-y')^2]^{1/2}}, \tag{3}$$

where both the field point (x,y) and the source point (x',y') are on contours C_a and C_c.

An integral equation for $\phi_1(x,y)$ can be derived by multiplying (1) by G_0 and (2) by ϕ_1. Then if these equations are summed;

$$G_0\,\nabla^2\,\phi_1 - \phi_1\,\nabla^2\,G_0 = \delta\phi_1. \tag{4}$$

If both sides of (4) are integrated over the volume bounded by $C_a + C_c$, Green's theorem can be applied to obtain the relation:

$$\phi_1(x,y) = \int_{C_a+C_c}\left[G_0\frac{\partial\phi_1}{\partial n} - \phi_1\frac{\partial G_0}{\partial n}\right]dS. \tag{5}$$

In region II, the same procedure can be applied to obtain:

$$\phi_2(x,y) = \int_{C_b-C_c}\left[G_0\frac{\partial\phi_2}{\partial n} - \phi_2\frac{\partial G_0}{\partial n}\right]dS. \tag{6}$$

In region III, the integral equation solution for Poisson's equation in terms of the source ρ_s becomes:

$$\phi_3(x,y) = \frac{1}{\epsilon_3}\int_{C_1}\rho_{s1}G_0\,dS + \frac{1}{\epsilon_3}\int_{C_2}\rho_{s2}G_0\,dS - \int_{C_a+C_b+C_0}\left[G_0\frac{\partial\phi_3}{\partial n} - \phi_3\frac{\partial G_0}{\partial n}\right]dS. \tag{7}$$

A set of equations describing the potential everywhere can then be obtained from (5), (6) and (7) as follows:
For region I:

$$\phi_1(x,y) = \int_{C_a+C_c}\left[G_0\frac{\partial\phi_1}{\partial n} - \phi_1\frac{\partial G_0}{\partial n}\right]dS, \quad (x,y)\in \text{I}. \tag{8}$$

and

$$0 = \int_{C_a+C_c}\left[G_0\frac{\partial\phi_1}{\partial n} - \phi_1\frac{\partial G_0}{\partial n}\right]dS, \quad (x,y)\in \text{II or III}. \tag{9}$$

For region II:

$$\phi_2(x,y) = \int_{C_b-C_c}\left[G_0\frac{\partial\phi_2}{\partial n} - \phi_2\frac{\partial G_0}{\partial n}\right]dS, \quad (x,y)\in \text{II} \tag{10}$$

and

$$0 = \int_{C_b-C_c}\left[G_0\frac{\partial\phi_2}{\partial n} - \phi_2\frac{\partial G_0}{\partial n}\right]dS, \quad (x,y)\in \text{I or III}. \tag{11}$$

For region III:

$$\phi_3(x,y) = \frac{1}{\epsilon_3}\int_{C_1}\rho_{s1}G_0\,dS + \frac{1}{\epsilon_3}\int_{C2}\rho_{s2}G_0\,dS - \int_{C_a+C_b+C_0}\left[G_0\frac{\partial\phi_3}{\partial n} - \phi_3\frac{\partial G_0}{\partial n}\right]dS, \quad (x,y)\in \text{III} \tag{12}$$

and

$$0 = \frac{1}{\epsilon_3}\int_{C_1}\rho_{s1}G_0\,dS + \frac{1}{\epsilon_3}\int_{C_2}\rho_{s2}G_0\,dS - \int_{C_a+C_b+C_0}\left[G_0\frac{\partial\phi_3}{\partial n} - \phi_3\frac{\partial G_0}{\partial n}\right]dS, \quad (x,y)\in \text{I or II}. \tag{13}$$

The potentials in (9), (11), and (13) vanish because the regions of integration do not contain the delta function from the Green's function relation in (2). If the contour C_0 is assumed to approach infinity, the integration on that contour does not contribute to the solution.

Equations (8) through (13) are combined by using the boundary condition $\phi_1 = \phi_2$ on $C_c, \phi_2 = \phi_3$ on C_b and $\phi_1 = \phi_3$ on C_a, which leads to one equation valid for regions I, II and III, i.e.:

$$\phi_i(x,y) = \frac{1}{\epsilon_3}\int_{C_1}\rho_{s1}G_0\,dS + \frac{1}{\epsilon_3}\int_{C_2}\rho_{s2}G_0\,dS + \int_{C_a}G_0\left[\frac{\partial\phi_1}{\partial n} - \frac{\partial\phi_3}{\partial n}\right]dS + \int_{C_b}G_0\left[\frac{\partial\phi_2}{\partial n} - \frac{\partial\phi_3}{\partial n}\right]dS + \int_{C_c}G_0\left[\frac{\partial\phi_1}{\partial n} - \frac{\partial\phi_2}{\partial n}\right]dS, \quad (x,y)\in i \tag{14}$$

where i = I, II or III.

Since the integrand of the potential integral equation is discontinuous on C_t, it can be represented in terms of three equivalent surface charge densities. Thus, this three-dielectric region problem can be represented in terms of two sources, ρ_{s1} and ρ_{s2}, and three surface charge densities, σ_a, σ_b and σ_c, residing on the interfaces of homogenous media C_a, C_b and C_c, respectively. Therefore equation (14) reduces to

$$\phi_i(x,y) = \frac{1}{\epsilon_0}\int_{C_1}\rho_{s1}G_0\,dS + \frac{1}{\epsilon_0}\int_{C_2}\rho_{s2}G_0\,dS + \frac{1}{\epsilon_0}\int_{C_a}\sigma_a G_0\,dS + \frac{1}{\epsilon_0}\int_{C_b}\sigma_b G_0\,dS + \frac{1}{\epsilon_0}\int_{C_c}\sigma_c G_0\,dS, \quad (x,y)\in i \tag{15}$$

where ϵ_3 is replaced by ϵ_0.

For this mathematical model, the normal component of the displacement vector $\boldsymbol{D}$ is continuous on the contours separating the regions. This condition leads to another integral equation in terms of equivalent surface charges. If the derivative of (15) in the appropriate region is taken and the condition

$$\epsilon_2\left(-\frac{\partial\phi_2}{\partial n}\right) - \epsilon_1\left(-\frac{\partial\phi_1}{\partial n}\right) = 0, \quad (x,y)\in C_c \tag{16}$$

is enforced, along with the extraction of the principal value for the improper integral as the field point (x,y) approaches the contour C_c, another integral equation can be obtained [12]. After some mathematical manipulations, the application of (16) gives the following three integral equations:

$$(\epsilon_{r1}-\epsilon_{r2})\left[\int_{C_1}\rho_{s1}\frac{\partial G_0}{\partial n}dS + \int_{C_2}\rho_{s2}\frac{\partial G_0}{\partial n}dS + \int_{C_a}\sigma_a\frac{\partial G_0}{\partial n}dS + \int_{C_b}\sigma_b\frac{\partial G_0}{\partial n}dS + \int_{C_c}\sigma_c\frac{\partial G_0}{\partial n}dS\right] + (\epsilon_{r1}+\epsilon_{r2})\frac{\sigma_c}{2} = 0, \quad (x,y)\in C_c, \tag{17}$$

and

$$(\epsilon_{r1}-1)\left[\int_{C_1}\rho_{s1}\frac{\partial G_0}{\partial n}dS + \int_{C_2}\rho_{s2}\frac{\partial G_0}{\partial n}dS + \int_{C_a}\sigma_a\frac{\partial G_0}{\partial n}dS + \int_{C_b}\sigma_b\frac{\partial G_0}{\partial n}dS + \int_{C_c}\sigma_c\frac{\partial G_0}{\partial n}dS\right] + (\epsilon_{r1}+1)\frac{\sigma_a}{2} = 0, \quad (x,y)\in C_a, \tag{18}$$

$$(\epsilon_{r2}-1)\left[\int_{C_1}\rho_{s1}\frac{\partial G_0}{\partial n}dS + \int_{C_2}\rho_{s2}\frac{\partial G_0}{\partial n}dS + \int_{C_a}\sigma_a\frac{\partial G_0}{\partial n}dS + \int_{C_b}\sigma_b\frac{\partial G_0}{\partial n}dS + \int_{C_c}\sigma_c\frac{\partial G_0}{\partial n}dS\right] + (\epsilon_{r2}+1)\frac{\sigma_b}{2} = 0, \quad (x,y)\in C_b, \tag{19}$$

where $\epsilon_1 = \epsilon_{r1}\epsilon_0$ and $\epsilon_2 = \epsilon_{r2}\epsilon_0$.

In order to specialize the general geometry in Fig. 2 to the microstrip problem shown in Fig. 1, the contours C_1 and C_2 will touch C' and C''', respectively. The normal component of the displacement vector $\boldsymbol{D}$ is then discontinuous by an amount equal to the free-charge density on the conductors. This discontinuity condition results in the following equation:

$$(\epsilon_{r1}-1)\left[\int_{C_1}\rho_{s1}\frac{\partial G_0}{\partial n}dS + \int_{C_2}\rho_{s2}\frac{\partial G_0}{\partial n}dS + \int_{C_a}\sigma_a\frac{\partial G_0}{\partial n}dS + \int_{C_b}\sigma_b\frac{\partial G_0}{\partial n}dS + \int_{C_c}\sigma_c\frac{\partial G_0}{\partial n}dS\right] + (\epsilon_{r1}+1)\frac{\sigma_a}{2} + (\epsilon_{r1}-1)\frac{\rho_{s1}+\rho_{s2}}{2} = 0, \quad (x,y)\in C' \text{ or } C'''. \tag{20}$$

Equations (15), (17), (18), (19) and (20) represent a set of integral equations which can be used to solve for the unknown charge densities $\rho_{s1}, \rho_{s2}, \sigma_a, \sigma_b$ and σ_c, with known potential ϕ_{c1} and ϕ_{c2} on the conductive contours C_1 and C_2. These equations can be reduced to a set of matrix equations by using the method of moments. Pulse basis function and point matching techniques using Dirac delta functions for testing are employed for the numerical solution [2], [12].

After these charge densities are obtained, the capacitances, C_{11}, C_{12}, C_{21} and C_{22} are easily derived. The characteristics

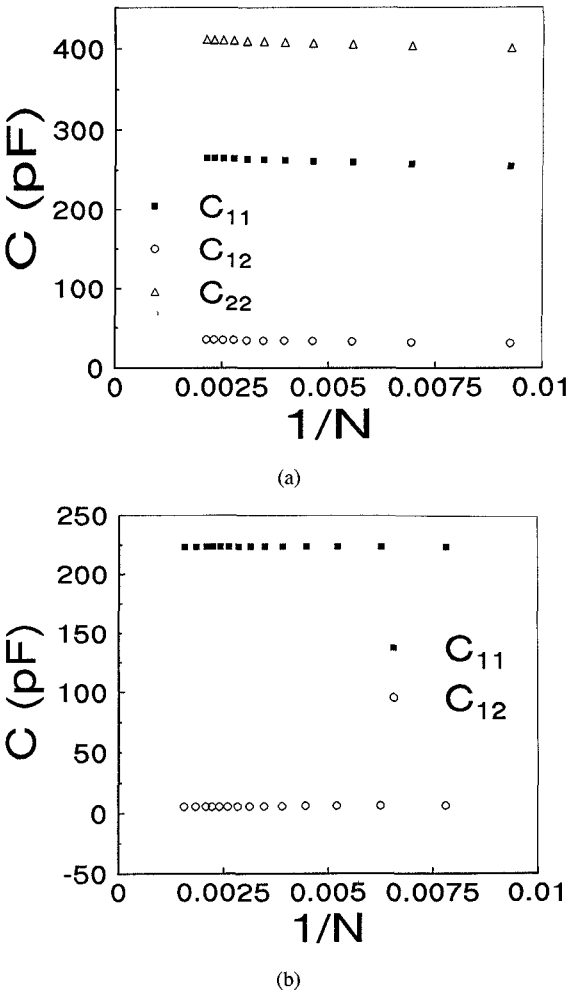

Fig. 3. Convergence of capacitances. (a) Asymmetric. (b) Symmetric.

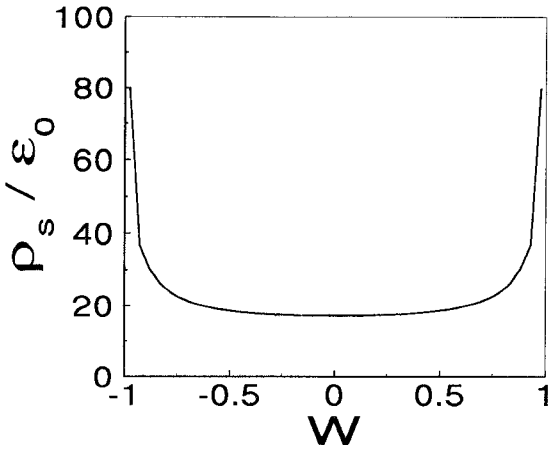

(a)

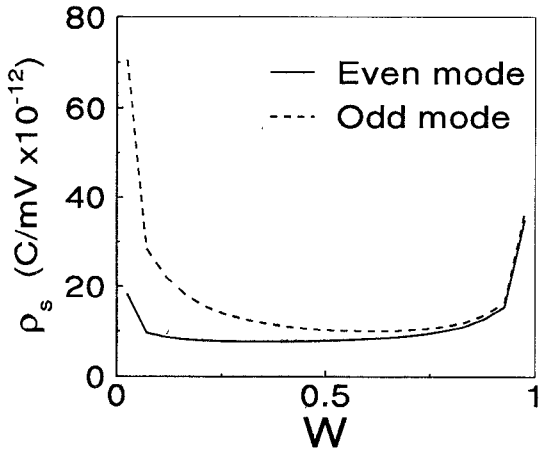

(b)

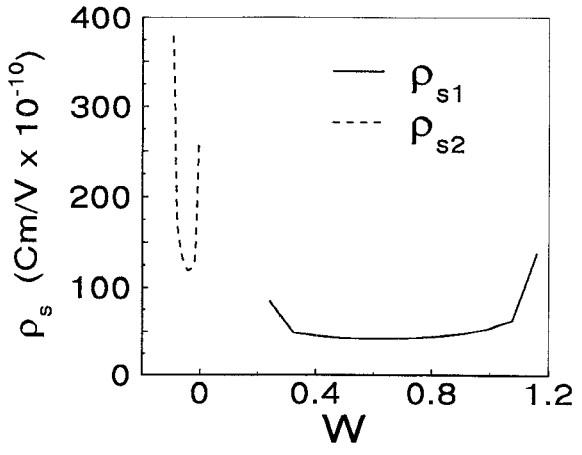

(c)

Fig. 4. Charge distributions. (a) Single strip transmission line. (b) Symmetric transmission line. (c) Asymmetric transmission line.

impedances, relative permittivities, and phase velocities are also computed based on the definitions in [11].

III. Numerical Results and Discussion

A general computer program has been written to obtain numerical solutions for the microstrip transmission line shown in Fig. 1. After these charge densities are obtained, the capacitances of an asymmetric two-conductor microstrip transmission line and all other parameters, such as characteristic

TABLE I
Comparison of Computed Results with those in [13] for $B/H = 0.2, \epsilon_{r1} = 10, T/W = 5$

		This work	From [13]
W/H=1.0	C_{11} (pF/m)	141.48	141.77
	C_{12} (pF/m)	56.44	57.56
	ϵ_{ee}	7.222	7.209
	ϵ_{eo}	5.713	5.699
	V_e (10^8m/s)	1.1164	1.1165
	V_o (10^8m/s)	1.2551	1.2558
	Z_{oe} (ohm)	63.31	63.18
	Z_{oo} (ohm)	31.32	31.00
W/H=2.0	C_{11} (pF/m)	230.53	231.60
	C_{12} (pF/m)	56.47	59.95
	ϵ_{ee}	7.786	7.777
	ϵ_{eo}	6.042	6.020
	v_e (10^8m/s)	1.0751	1.0750
	v_o (10^8m/s)	1.2205	1.2219
	Z_{oe} (ohm)	40.35	40.17
	Z_{oo} (ohm)	23.85	23.28

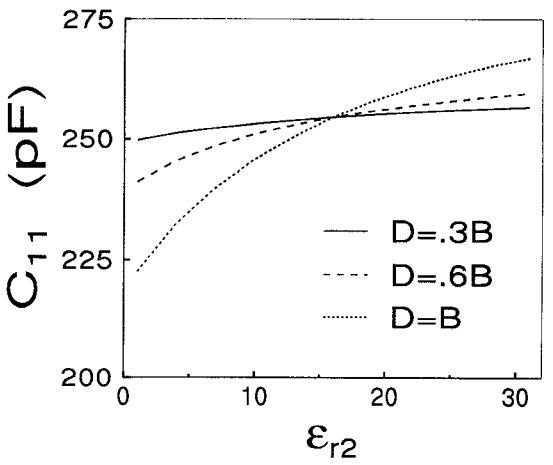

(a)

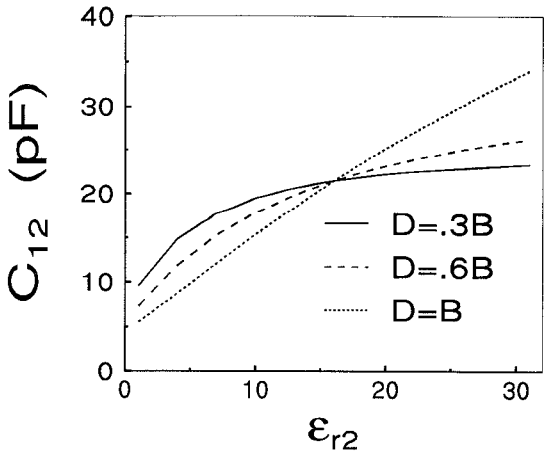

(b)

Fig. 5. Capacitances versus ϵ_{r2} for $L = 0.6H$. (a) C_{11}. (b) C_{12}.

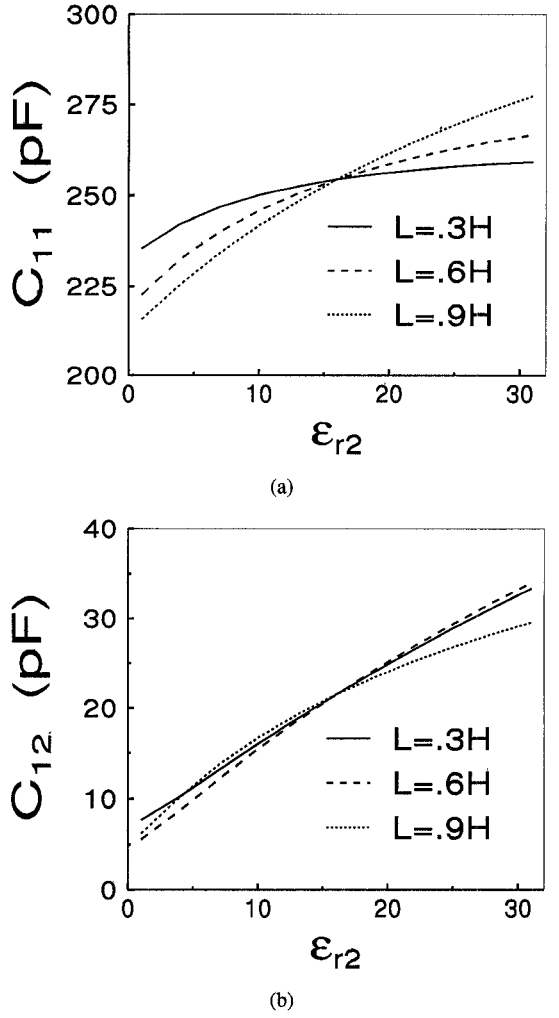

Fig. 6. Capacitances versus ϵ_{r2} for $D = B$. (a) C_{11}. (b) C_{12}.

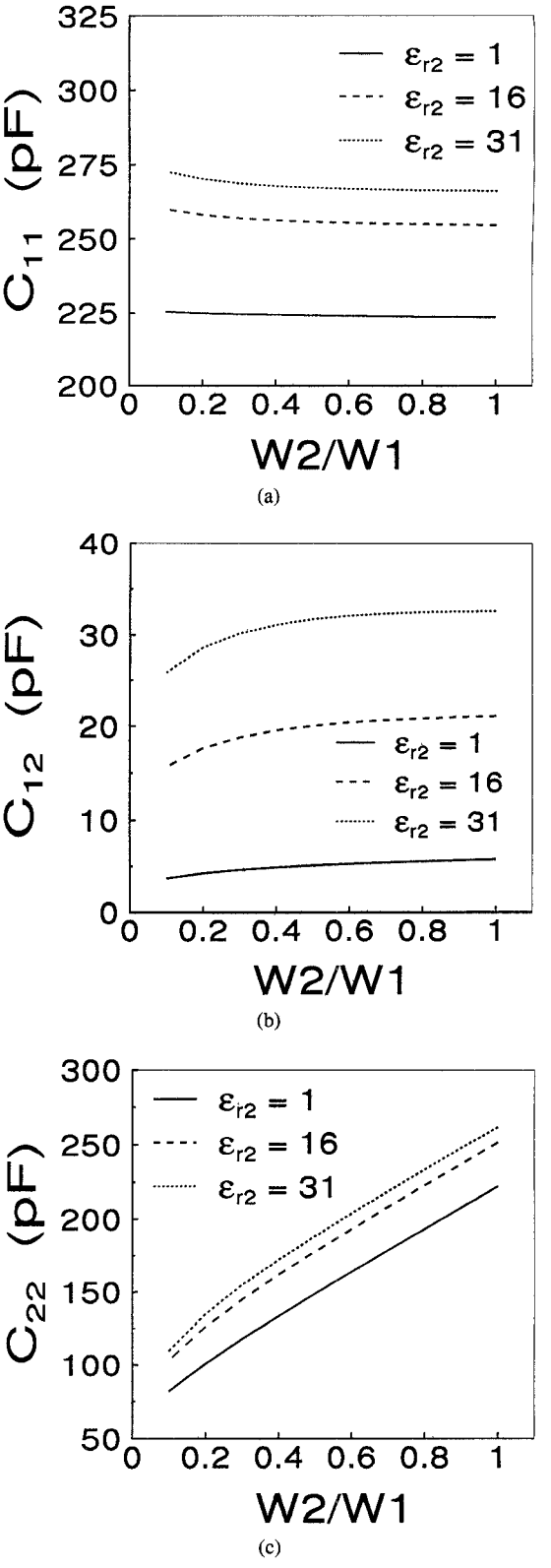

Fig. 7. Capacitances versus $W2/W1$. (a) C_{11}. (b) C_{12}. (c) C_{22}.

impedances, phase velocities, and effective permittivities for a symmetric microstrip transmission line, are determined.

The convergence of our numerical solution can be observed in Fig. 3(a) and (b) for asymmetric and symmetric transmission lines, respectively. In these figures the capacitances based on the configuration shown in Fig. 1 versus N which is the order of matrix involved in the solution with equal segments for the expansion functions are shown. In Fig. 3(a), $W_1/H = 1, W_2/W_1 = 2, D/B = 1, L/H = 0.6, B/H = 1, T/W_1 = 5, \epsilon_{r1} = 16$ and $\epsilon_{r2} = 31$. For this asymmetric transmission line, the relative percentage error between the extrapolated and computed values of the capacitances in this study, with $N = 480$, for C_{11} is about 1.5%, for C_{12} (or C_{21}) is about 4.1% and for C_{22} is about 0.96%. Fig. 3(b) shows the convergence of the capacitances based on the best decoupling parameters for a symmetric transmission line defined by $W_1/H = 1, W_2/W_1 = 1, D/B = 1, L/H = 0.6, B/H = 1, T/W_1 = 5, \epsilon_{r1} = 16$ and $\epsilon_{r2} = 1$. The relative percentage error between the extrapolated and the computed values, with $N = 640$, for C_{11} (or C_{22}) is about 0.16% and for C_{12} (or C_{21}) is about 4.7%.

In order to verify the numerical results generated by the computer code, comparisons of few cases with published data have been made. Fig. 4(a) shows the surface charge on a single strip transmission line which is a limiting case of the two conductor transmission line by setting $L = 0$ and $B = 0$ with $W = W_1 = W_2, W/H = 1, \epsilon_{r1} = 16$ and $T/W = 5$. The charge distribution in the figure is in good agreement with those in Fig. 3 in [6]. In the figure, the

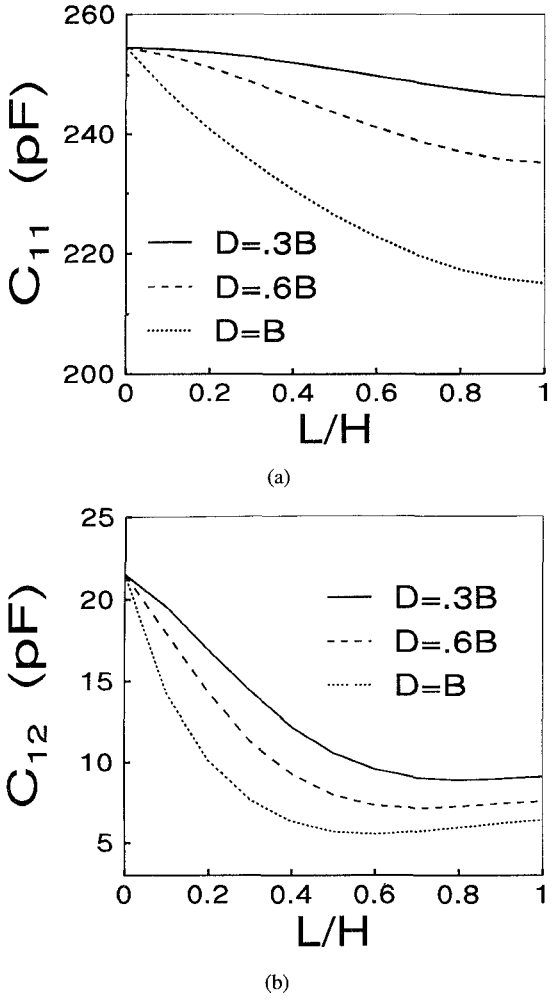

Fig. 8. Capacitances versus L/H. (a) C_{11}. (b) C_{12}.

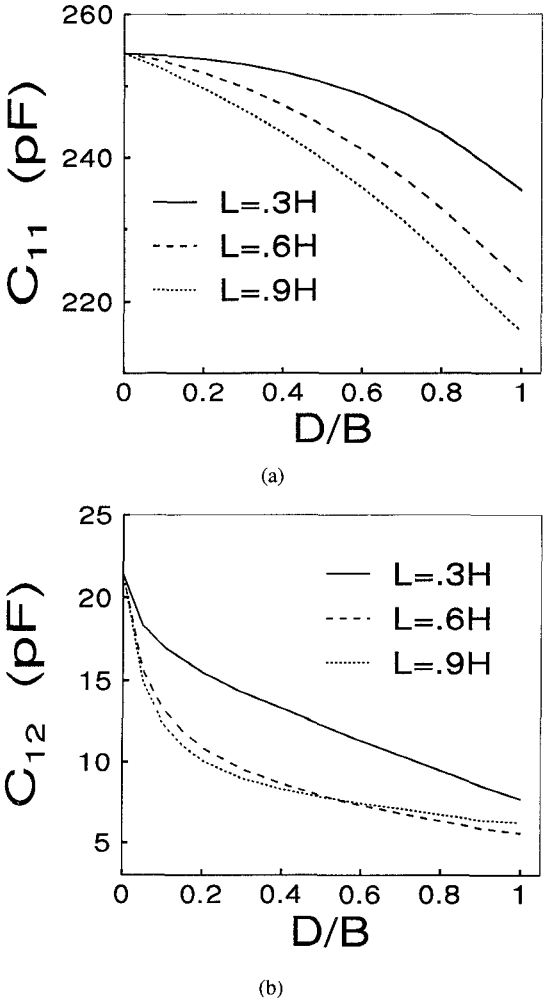

Fig. 9. Capacitances versus D/B. (a) C_{11}. (b) C_{12}.

charge density is normalized by ϵ_0, in order to compare with the data in [6]. Fig. 4(b) shows the charge distributions for the even and odd modes of a symmetric line with $\epsilon_{r1} = 16, B/H = 0.3, L = 0$, and $W/H = 1$. These charges match those in Fig. 9 in [13]. The charge distribution on an asymmetric transmission line are shown in Fig. 4(c), for $W_1/H = 1, W_2/W_1 = 0.1, B/H = 0.2, L = 0$, and $\epsilon_{r1} = 9$. The computed charge, as shown, agrees with those reported in Fig. 7 in [8]. Table I gives a comparison of the computed line characteristic parameters with previously reported results [13] for a symmetric transmission line with $\epsilon_{r1} = 10, B/H = 0.2, T/W = 5$ and $L = 0$, which again indicates very good agreement. Another attempt to validate the computer code has been made by computing a two-conductor microstrip transmission line without the notch, which is obtained by letting $\epsilon_{r2} = \epsilon_{r1}$, where D and L can be any value satisfying the relations $D \leq B$ and $L \leq H$ which gave the same numerical results, although not shown here.

With the developed program, the transmission line parameters of the geometry in Fig. 1 such as self and mutual capacitances, characteristic impedance, phase velocity, and effective permittivity are studied. With $W/H = 1, T/W = 5, B/H = 1$ and $\epsilon_{r1} = 16$, the effects of D, L and ϵ_{r2} on the self and mutual capacitances between these two strips are shown in Figs. 5 and 6. Fig. 5 shows the capacitances C_{11} and C_{12} versus ϵ_{r2} for $L = 0.6H$ and D is a varying parameter, while Fig. 6 shows the capacitances C_{11} and C_{12} versus ϵ_{r2} for $D = B$ and L is a varying parameter. In order to investigate the decoupling between the strips, the mutual-capacitance C_{12} (or C_{21}) is the most important factor to be discussed. As can be seen, there is an intersection between the curves in these figures. This occurs when $\epsilon_{r2} = 16$ (i.e., $\epsilon_{r2} = \epsilon_{r1}$), which means that there is no notch between the two strips. At this point, the capacitances should have the same values because the geometry is the same. From Figs. 5(b) and 6(b), it can be seen that C_{12} increases with ϵ_{r2}. This means that the minimum can be obtained when $\epsilon_{r2} = 1$, which represents

TABLE II
THE PARAMETERS FOR MINIMUM COUPLING

T	ϵ_{r1}	H	B	W2	W1	ϵ_{r2}	D	L
5.0	16	1.0	1.0	1.0	1.0	1	1.0	0.6
5.0	16	1.0	1.0	2.0	1.0	1	1.0	0.6
5.0	16	1.0	0.5	1.0	1.0	1	0.5	0.7
5.0	16	0.5	1.0	1.0	1.0	1	1.0	0.2
5.0	4.7	1.0	1.0	1.0	1.0	1	1.0	0.5
2.0	16	1.0	1.0	1.0	1.0	1	1.0	0.6

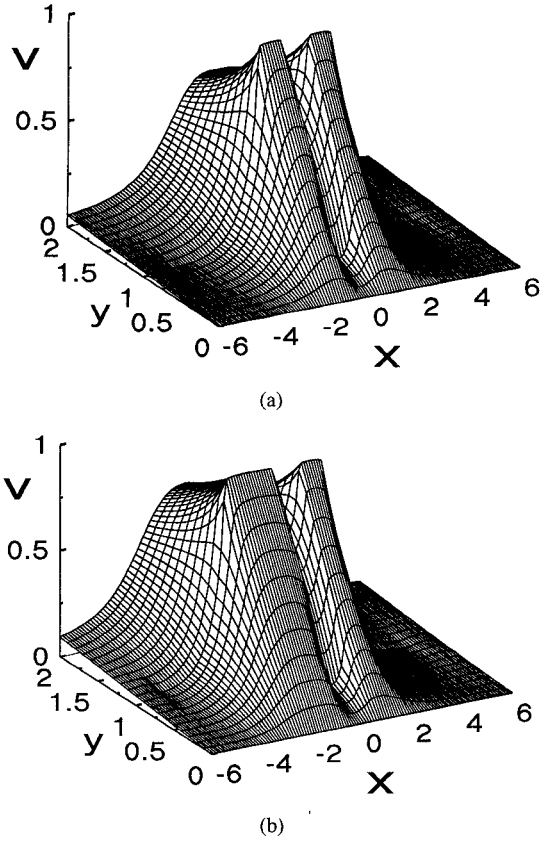

(a)

(b)

Fig. 10. Potential distribution for even mode. (a) For first row in Table II. (b) For second row in Table II.

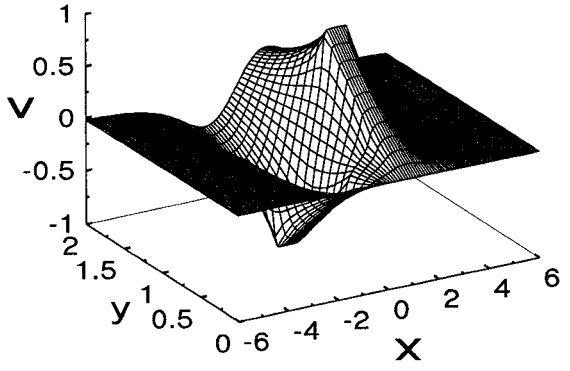

(a)

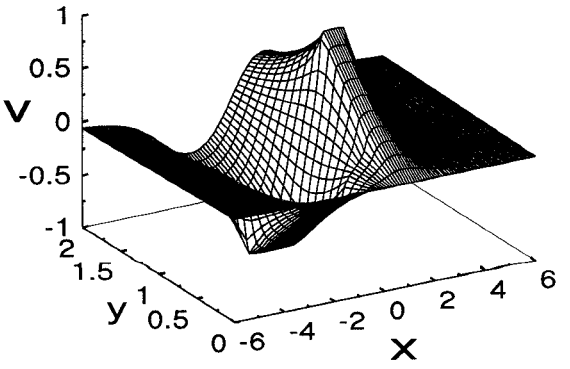

(b)

Fig. 11. Potential distribution for odd mode. (a) For first row in Table II. (b) For second row in Table II.

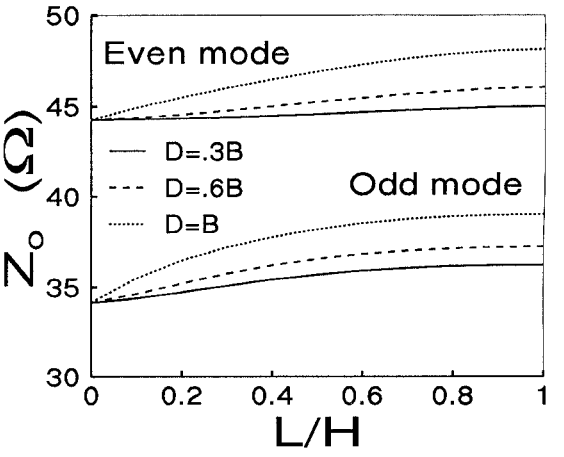

(a)

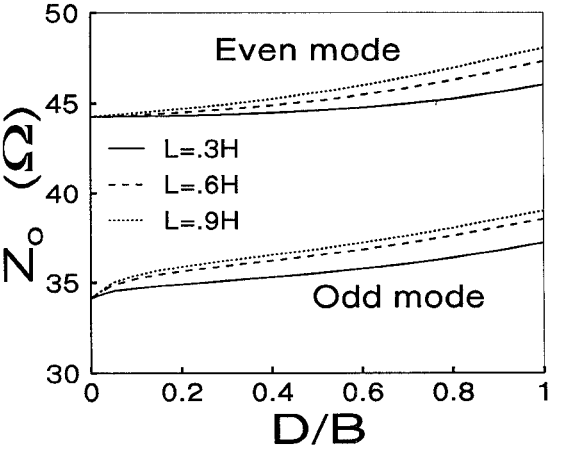

(b)

Fig. 12. Characteristic impedances. (a) Z_o versus L/H. (b) Z_o versus D/B.

the air-dielectric notch. This property shows that a possible method for reducing the coupling between the strip lines is by removing a rectangular material from the substrate between the conductors. Fig. 7 shows the effects of changing the width of one strip on the capacitances for various value of ϵ_{r2}, where $W1 = H, T/W = 5, L = 0.6H, B = H$, and $\epsilon_{r1} = 16$. It is clear that ϵ_{r2} should be 1 in order to get the best decoupling.

Then, consider a symmetric geometry where $W/H = 1, T/W = 5, B/H = 1, \epsilon_{r1} = 16$ and ϵ_{r2} is fixed to be 1 which leads to a removed rectangular dielectric notch. The influences of various D and L on the self and mutual capacitances between the strips are shown in Figs. 8 and 9. Fig. 8 shows the influences of various L with different D, while Fig. 9 shows the influences of various D with different L. After studying these figures, some important properties can be seen. From Fig. 9(b), it can be easily seen that for best decoupling D should be equal to B which means that, the width of the material to be removed between the lines should be as wide as possible. Furthermore, from Fig. 8(b), the curve which represents $D = B$ shows a minimum value for L/H. This means, that for best decoupling the depth of the material to be removed between the lines should be approximately $L/H = 0.6$. Thus, for best decoupling, $D = B$ and $L \cong 0.6H$ for this microstrip line. It can be also shown in Figs. 8 and 9,

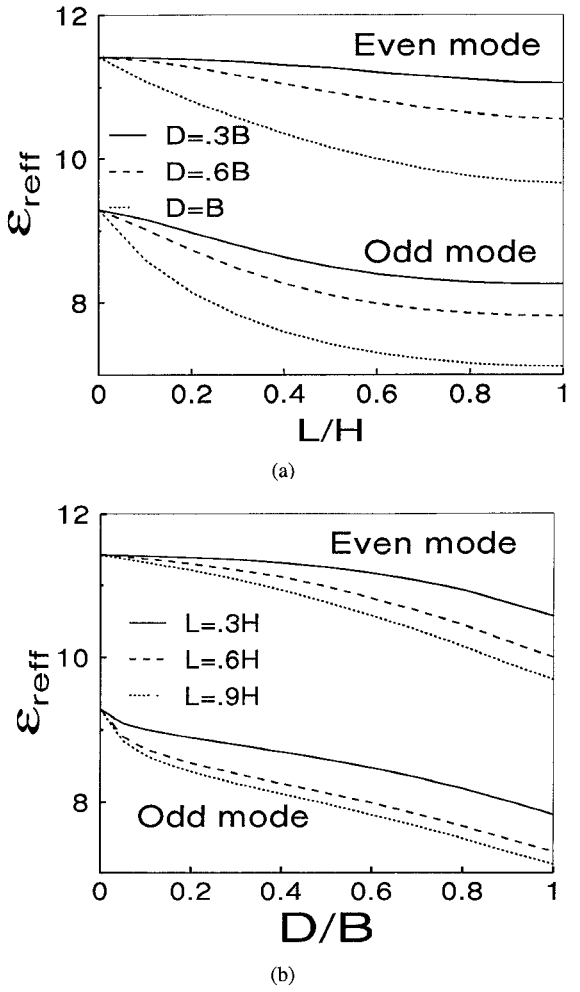

Fig. 13. Relative effective permittivities. (a) ϵ_{reff} versus L/H. (b) ϵ_{reff} versus D/B.

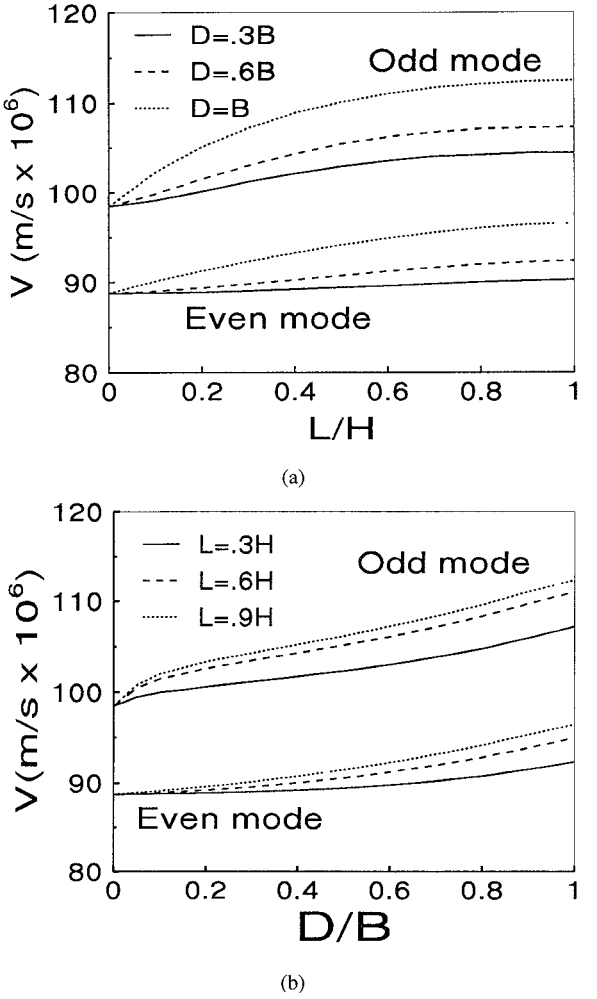

Fig. 14. Phase velocities. (a) V versus L/H. (b) V versus D/B.

that removing a dielectric notch forces the mutual-capacitance to decrease significantly, however, the self-capacitances do not show significant percentage variations.

The parameters for minimum coupling between the strips for six different geometries of the microstrip transmission line are computed and listed in Table II. Fig. 10(a) and (b) show the potential distribution around the conducting strips for transmission lines characterized by the parameters in the first and second rows in Table II, respectively, when both strips are charged to 1 V (even mode). Whereas Fig. 11(a) and (b) show the corresponding potentials when one strip is charged to 1 V and the other is charged to -1 V (odd mode).

Furthermore, the influences on the characteristic impedances, effective permittivities and phase velocities are studied for even and odd modes of a symmetric transmission line with $W1 = W2 = H, T/W1 = 5, B/H = 1, \epsilon_{r1} = 16$ and $\epsilon_{r2} = 1$. Fig. 12–14 show the characteristic impedances (Z_o), the relative effective permittivity (ϵ_{reff}) and the phase velocities (V) for even and odd modes versus L/H and D/B. It has been found that all these parameters do not significantly change, in relative percentages, compared with the changes in the mutual-capacitance. Because the phase velocities for both modes appear to change in the same proportion, the coupling frequency characteristics will be the same as a related standard microstrip directional coupler [14].

IV. Conclusion

A numerical solution for the analysis of a two-conductor microstrip transmission line with a rectangular dielectric notch between two conducting strips is presented. The procedure consists of formulating the necessary three media integral equations for the numerical solution for the charge distributions. The decoupling between such two-conductor microstrip transmission line is investigated. The solution is based on a quasi-TEM approach where the thickness of the conductors is assumed to be zero.

The coupling between circuit interconnections limits the bandwidth of dense microwave circuits and logic speed of digital and computing circuits and systems. It has been shown in this study that the coupling between two conducting lines is minimized by removal of the dielectric material between the lines. The mututal-capacitance varies significantly when this method is employed. With the removal of a rectangular shaped material, it is found that the width should be as wide as possible between the conducting lines but the depth should have an optimum value depending on the remaining param-

eters. One example has been given for symmetric microstrip transmission line.

This knowledge related to the physics of the interconnecting line decoupling for dense integrated and microstrip circuits is useful in the design and development of faster IC chips and broader bandwidth microwave circuits for communications required in future microwave and millimeter wave systems.

REFERENCES

[1] A. E. Ruehli, "Survey of computer-aided electrical analysis of integrated circuit interconnections," *IBM J. Res. Development*, vol. 23, no. 6, pp. 626–639, Nov. 1979.

[2] R. F. Harrington, *Field Computation by Moment Methods*. New York: Macmillan, 1968.

[3] R. F. Harrington and K. Pontoppidan, "Computation of Laplacian potentials by an equivalent source method," *Proc. Inst. Elec. Eng.*, vol. 116, no. 10, pp. 1715–1720, Oct. 1969.

[4] A. T. Adams and J. R. Mautz, "Computer solution of electrostatic problem by matrix inversion," in *Proc. Nat. Electronics Conf.*, vol. 25, pp. 198–201, Dec. 1969.

[5] C. E. Smith, "A coupled integral equation solution for microstrip transmission lines," in *IEEE G-MTT Microwave Symp. Dig.*, June 1973, pp. 284–286.

[6] C. E. Smith and R. S. Chang, "Microstrip transmission lines with finite-width dielectric," *IEEE Trans. Microwave Theory Tech.*, vol. MTT-28, pp. 90–94, Feb. 1980.

[7] C. E. Smith and R. S. Chang, "Microstrip transmission lines with finite-width dielectric and ground plane," *IEEE Trans. Microwave Theory Tech.*, vol. MTT-33, pp. 835–839, Sept. 1985.

[8] S. Bokka, "Computation of electrical characteristics of asymmetric microstrip multiconductor transmission lines," M.S. thesis, University of Mississippi, University, MI, May 1980.

[9] V.K. Tripathi, "Asymmetric coupled transmission lines in a inhomogeneous medium," *IEEE Trans. Microwave Theory Tech.*, vol. MTT-23, pp. 734–738, Sept. 1975.

[10] D. Kajfez, "Quasi-TEM modes on coupled transmission lines with asymmetric conductors," *Electrotechnical Review*, vol. 44, no. 1, pp. 1–9, 1977.

[11] D. Kajfez, *Notes on Microwave Circuits*. vol. 2, ch. 7, "Multiconductor transmission lines," Kajfez Consulting, Oxford, MS, 1986.

[12] S. He, A. Z. Elsherbeni, and C. E. Smith, "Analysis of two-conductor microstrip transmission line with a dielectric overlay," Tech. Rep., Department of Electrical Engineering, University of Mississippi, University, MS, Dec. 1991.

[13] T. G. Bryant and J. A. Weiss, "Parameters of microstrip transmission lines and coupled pair of microstrip lines," *IEEE Trans. Microwave Theory Tech.*, vol. MTT-16, pp. 1021–1027, Dec. 1968.

[14] T. C. Edward, *Foundations For Microstrip Circuit Design*, New York: Wiley, 1981, chapter 6.

Shidong He was born in Shanghai, China, on Dec. 22, 1961. He received the B.S. degree in electrical engineering from Shanghai Jiao Tong University, China, in 1984, and the M.S. degree in engineering science-electrical engineering from the University of Mississippi in 1991.

He first joined Shanghai Radio and TV Bureau, China, in 1984. Currently, he is an Availability Specialist in International Business Machines Corporation (IBM).

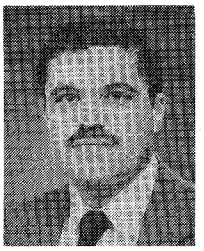

Atef Z. Elsherbeni (S'84–M'86–SM'91) was born in Cairo, Egypt on Jan. 8, 1954. He received the B.Sc. degree (with honors) in electronics and communications, the B.Sc. degree (with honors) in the applied physics, and the M.Eng. degree in electrical engineering, all from Cairo University, Cairo, Egypt, in 1976, 1979, and 1982, respectively. He received the Ph.D. degree in electrical engineering from Manitoba University, Winnipeg, MB, Canada, in 1987.

He was a Research Assistant with the Faculty of Engineering at Cairo University from 1976 to 1982, and from 1983 to 1986 at the Electrical Engineering Department, Manitoba University and from Jan. to Aug. 1987 as a Post Doctoral Fellow in the same department. He joined the faculty at the University of Mississippi in Aug. 1987 where he is currently an Associate Professor of Electrical Engineering. His professional interests include microstrip antennas, scattering and diffraction of electromagnetics waves, numerical techniques and computer applications for electromagnetics education. He has authored and/or co-authored over 75 technical papers and reports on applied electromagnetics, antenna design, and microwave subjects.

Dr. Elsherbeni is a member of the IEEE Antennas and Propagation, the Microwave Theory and Techniques and the Magnetics Societies. His honorary memberships include the Electromagnetics Academy and the Scientific Sigma Xi Society.

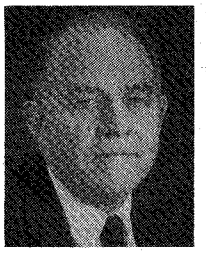

Charles E. Smith (S'59–M'68–SM'83) was born in Clayton AL, on June 8, 1934. He received the B.E.E. (with honors), M.S., and Ph.D. degrees from Auburn University Auburn, AL, in 1959, 1963, and 1968, respectively.

While pursuing his advanced degrees from 1959 to 1968, he was employed as a Research Assistant with the Auburn University Research Foundation. In late 1968, he accepted a position of Assistant Professor of Electrical Engineering with the University of Mississippi, University, MS, and he advanced to the rank of Associate Professor in 1969. He was appointed Chairman of the Department of Electrical Engineering in 1975, and he is currently Professor and Chair of this department. His main areas of interest are related to the application of electromagnetic theory to numerical methods, electrical properties of materials, automated EM measurements, microwave circuits, CAD, and antennas. His current research is related to computer-aided-design of ultra-fast or broadband VSLI and MMIC circuits, the characterization of electrical properties of materials using probes, and electromagnetic sensors for robots and other automated systems.